Optical Materials 73 (2017) 400–407

Contents lists available at ScienceDirect

Optical Materials

journal homepage: www.elsevier.com/locate/optmat

Signal intensity enhancement of laser ablated volume holograms

J.M. Versnel [a, *], C. Williams [b], C.A.B. Davidson [a], T.D. Wilkinson [b], C.R. Lowe [a]

[a] Institute of Biotechnology, Department of Chemical Engineering and Biotechnology, University of Cambridge, Cambridge CB3 0FA, United Kingdom
[b] Electrical Engineering Division, Department of Engineering, University of Cambridge, Cambridge CB2 1QT, United Kingdom

ARTICLE INFO

Article history:
Received 22 June 2017
Accepted 2 August 2017

Keywords:
Holographic sensor
Laser ablation
Holography
Diffraction
Optical devices
Metallic nanoparticles

ABSTRACT

Conventional volume holographic gratings (VHGs) fabricated in photosensitive emulsions such as gelatin containing silver salts enable the facile visualization of the holographic image in ambient lighting. However, for the fabrication of holographic sensors, which require more defined and chemically-functionalised polymer matrices, laser ablation has been introduced to create the VHGs and thereby broaden their applications, although the replay signal can be challenging to detect in ambient lighting. When traditional photochemical bleaching solutions used to reduce light scattering and modulate refractive index within the VHG are applied to laser ablated volume holographic gratings, these procedures decrease the holographic peak intensity. This is postulated to occur because both light and dark fringes contain a proportion of metal particles, which upon solubilisation are converted immediately to silver iodide, yielding no net refractive index modulation. This research advances a hypothesis that the reduced intensity of holographic replay signals is linked to a gradient of different sized metal particles within the emulsion, which reduces the holographic signal and may explain why traditional bleaching processes result in a reduction in intensity. In this report, a novel experimental protocol is provided, along with simulations based on an effective medium periodic 1D stack, that offers a solution to increase peak signal intensity of holographic sensors by greater than 200%. Nitric acid is used to etch the silver nanoparticles within the polymer matrix and is thought to remove the smaller particles to generate more defined metal fringes containing a soluble metal salt. Once the grating efficiency has been increased, this salt can be converted to a silver halide, to modulate the refractive index and increase the intensity of the holographic signal. This new protocol has been tested in a range of polymer chemistries; those containing functional groups that help to stabilize the metal nanoparticles within the matrix yield more intense holographic signals as the integrity of the fringe is more protected with increasing metal solubility.

1. Introduction

Volume holographic gratings (VHGs) fabricated in photosensitive emulsions, such as silver halide salts within a gelatin emulsion, produce intense holographic signals that enable images to be detected visually in ambient lighting [1,2]. One limitation of these VHGs for use as sensors is the polymer matrix, which is normally hydrophilic and unable to detect analytes such as hydrocarbons, which require hydrophobic matrices for absorption. The use of laser ablation to generate VHGs in a wide range of hydrophilic and hydrophobic polymers, containing a variety of metal salts or dyes, has significantly broadened the application of such sensors [3–9]. Furthermore, a number of the steps currently used in photochemical processing can be eliminated to increase their cost-effectiveness [9,10]. Even so, their application can be limited, however, by the low intensity of the holographic signal in some polymer matrices, which makes visualization of sensor response challenging without the use of a spectrometer or a bright white light source. Traditional methods such as reversal or rehalogenation bleaches, used to increase signal intensity of photochemically produced VHGs, results in the loss of intensity in ablated holograms. This research advances a hypothesis to explain the loss of intensity associated with the use of these bleaching agents and provides an alternative post-processing regime to increase the peak intensity of ablated VHG sensors.

Whilst the exact mechanism that generates the volume

* Corresponding author.
E-mail address: jmv27@cam.ac.uk (J.M. Versnel).

http://dx.doi.org/10.1016/j.optmat.2017.08.003

diffraction grating within the emulsion is not fully understood, it is thought to result from an in situ reduction in the size of the metal particles and the formation of alternating light and dark fringes (high-low index modulation) [7]. The fabrication process begins with diffusion of a metal salt solution into a polymer matrix. If the choice of solvent is optimized for the polymer matrix, the metal salts are likely to diffuse homogenously through the depth of the polymer and on reduction, the metal nanoparticles are distributed randomly as a colloidal suspension. Following exposure from a coherent light source, metallic nanoparticles are arranged in periodic fringes to form a VHG [9].

The sensor response is linked to either a swelling of the polymer matrix and/or changes in refractive index, which generates a shift in wavelength and changes in intensity of the holographic signal [3–10]. If the polymer swells, either due to solvent being drawn into the polymer or electrostatic repulsion of charges, or there is an increase in refractive index, the diffracted light can be shifted to longer wavelengths. Likewise, a decrease in refractive index or a contraction of the polymer causes the diffracted light to be shifted to shorter wavelengths. The diffraction grating therefore acts as a reporter, and calibration of the holographic response enables accurate detection and quantification of the analyte using a spectrophotometer.

For the VHG recording, the grating vector, $\boldsymbol{K}_G$, is defined as, $\overrightarrow{\boldsymbol{K}_G} = \overrightarrow{\boldsymbol{k}_1} - \overrightarrow{\boldsymbol{k}_2}$, where $\boldsymbol{k}_1$ and $\boldsymbol{k}_2$ are the wavevectors of the interfering plane waves, as shown in Fig. 1(a). When the angle, 2θ, between these two waves $\rightarrow$ π, a reflection VHG is formed. The period of this sinusoidal fringe, Λ, is given by

$$\Lambda = m\frac{2\pi}{\left|\overrightarrow{\boldsymbol{K}_G}\right|} = \frac{m\lambda}{2\bar{n}\sin\left(\frac{2\theta}{2}\right)}$$

where $\bar{n}$ is the effective refractive index of the medium, m (integer) is the spectral order, λ is the illumination wavelength and $2\theta = \pi - \phi$. This will produce a sinusoidal modulation of the effective refractive index of the medium, the response of which is dependent on the material sensitivity. When illuminated with white light, the VHG selectively filters light according to the Bragg phase-matching condition, $\overrightarrow{\boldsymbol{K}_G} = \overrightarrow{\boldsymbol{k}_i} - \overrightarrow{\boldsymbol{k}_R}$, where $\boldsymbol{k}_i$ and $\boldsymbol{k}_R$ are the wavevectors of the incident and reflected waves, as shown in Fig. 1(b), with further details shown in ESI, Fig. S1.

Optimal narrowband reflection is achieved when the optical thickness of each layer in the stack is a quarter-wavelength. The strength of the holographic peak signal, formed by constructive interference of the partial reflections from each fringe plane, is dependent on the number of fringes and the modulation depth of the refractive index [11,12]. The effective refractive index of the high index fringes is highly dependent on both the particle size and fill fraction of the metal nanoparticles and an optimum set of parameters can be modelled to maximise grating efficiency and hence holographic intensity [12,13].

The main difference between VHGs produced by photochemical and laser ablation methods is the timing of the reduction of the

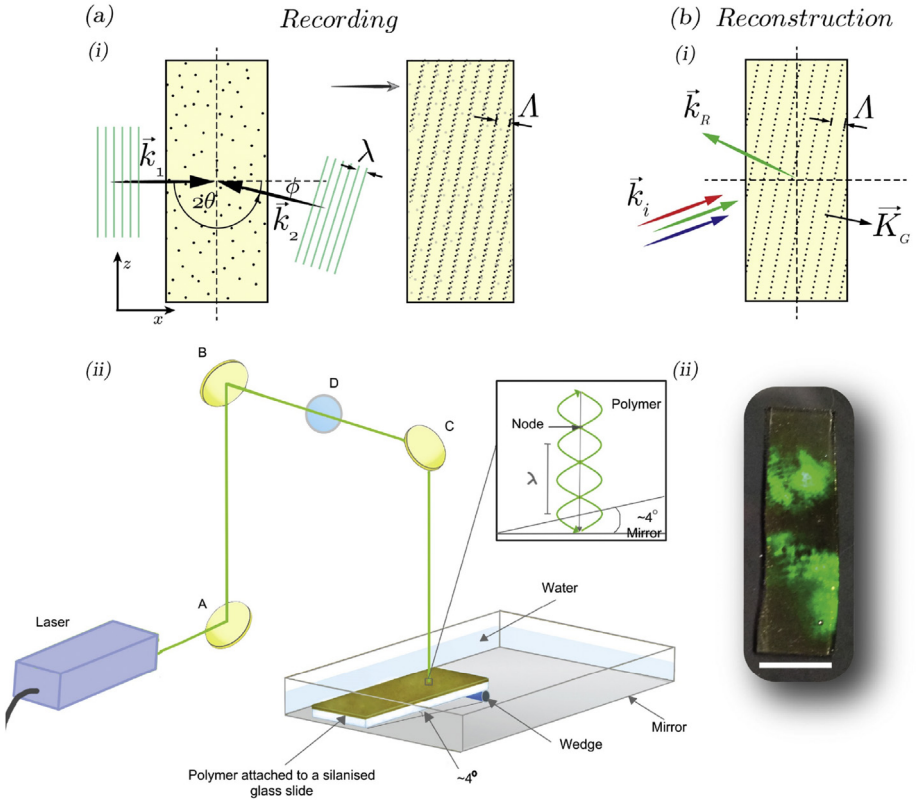

Fig. 1. Fabrication of Bragg reflection holograms. (a) Recording: (i) Schematic of holographic sensor recording process whereby the interference of two plane waves producing a periodic refractive index modulation of the medium. (ii) Nd:YAG pulsed laser generated a laser beam, which was directed by dichroic mirrors (A,B,C) and a spreader quartz lens (D), passed through the polymer and was reflected back by the mirror placed on the bottom of the plastic dish and running beneath the glass slide. The polymer on a silanised glass slide was placed on a 4° wedge lying on top of the mirror. The polymer was ablated either dry or immersed in deionised water to generate a hologram.(b) Reconstruction: (i) Reconstruction schematic highlighting the Bragg-phase matching condition. (ii) Photograph of a typical final sensor immersed in water bath, white scale bar ~3 cm.

silver halide colloidal solution and the post-processing steps. When photochemical methods are applied, the emulsion doped with silver halide salts is exposed to the laser before reducing the exposed areas; remaining silver halide salts are then washed out to yield alternating fringes with and without Ag^0 nanoparticles, which have been visualised using transmission electron microscopy [14,15]. Further increases in signal intensity can be achieved by post-exposure treatments, for example, rehalogenation or reversal bleaching, which reduces light scattering and modulates the refractive index. If the metal solution is reduced within the emulsion prior to laser irradiation, a VHG is fabricated by size ablation of Ag^0 nanoparticles throughout the matrix. It is hypothesised that the resultant peak signal intensity from the VHG is reduced compared to those fabricated photochemically due to the fact that there will be a distribution of sizes of nanoparticles within the matrix following laser ablation, thereby generating less defined fringes with light scattering superimposed on diffraction.

The presence of small metal particles in both the light and dark fringes is likely to scatter light, lower the efficiency of the grating and reduce the ability to further modulate refractive index. If laser ablated VHGs are bleached to silver halide salts there will be a subsequent increase in the size of the particles present in all fringes, and little potential for refractive index modulation. This can be likened to rehalogenation of an unfixed VHG fabricated using photochemical means, where the exposed areas contain Ag^0 nanoparticles and the unexposed regions contain silver bromide (AgBr). If a rehalogenation bleach is then applied, the Ag^0 particles in both the exposed and the unexposed regions become AgBr and the holographic signal is poor [16]. Silver is known to dissolve in the presence of nitric acid (HNO_3); the kinetics of these reactions is dependent on the size of the nanoparticle, the concentration of HNO_3 and the temperature of the reaction [17,18]. A relationship between nanoparticle size and the pH of a HNO_3 solution has been demonstrated, with particles less than 1.5 nm found at pH values between 1 and 2.5 [19]. If nitric acid is used to dissolve the smaller particles within both fringes post ablation, it should be possible to test this hypothesis. Whilst this treatment is likely to result in some loss of Ag^0 in both fringes, provided the fill fraction is not substantially reduced in the dark fringes, it should be possible to use a rehalogenation bleach to modulate refractive index and thereby holographic signal intensity. Similarly, if the hypothesis is correct, the use of hydrochloric acid, which has the potential to solubilise the Ag^0 and simultaneously convert it to silver chloride in one step should result in a decrease in holographic peak signal due to the fact that the process of removal of material did not occur before conversion to the silver halide salt. This report describes work designed to test these hypotheses.

2. Methods

2.1. Materials

2-Hydroxyethyl methacrylate (HEMA) (ultrapure >99%), ethylene glycol dimethacrylate (EDMA) (98%), N,N′-dimethylaminoethyl methacrylate (DMAEM) (99%), 2,2′-dimethoxy-2-phenylacetophenone (DMPA), 3-(trimethoxysilyl)propyl methacrylate, nitric acid (HNO_3), metol purum for holographic purposes (≥98%) and silver perchlorate ($AgClO_4$) were purchased from Sigma Aldrich Chemical Co., The Old Brick Yard, Gillingham, Dorset, U.K. Aluminized 100 μm polyester film MET401 was purchased from HiFi Industrial Film Ltd. (Stevenage, U.K.). Microscope slides (Super Premium, 1–1.2 mm thick, low iron) were purchased from BDH (Merck) Ltd.

2.2. Synthesis of polymer films

Glass microscope slides were placed in an aluminium tray to which a 2% (v/v) 3-(timethoxysilyl)propyl methacrylate in acetone solution was added and swirled over the slides to coat. Excess solution was removed and the slides were left in the dark to dry at room temperature (23 ± 3 °C). The slides were washed with ethanol followed by tap water and left to dry in air at (23 ± 3 °C) before addition of the polymer solution.

The polyHEMA-*co*-EDMA polymers were synthesised according to the protocol of Marshall et al. [5]. A 0.3 M silver perchlorate ($AgClO_4$) solution (300 μl) was pipetted onto the surface of a clean glass plate in a longitudinal strip. The glass slide, polymer side down, was placed onto the solution and left for 4min for the solution to diffuse into the polymer. The slide was then removed and excess solution wiped off and the polymer dried under a stream of hot air for 4–5s. The slide was then placed, polymer side up, in a bath of 1.5 M lithium bromide (LiBr) solution and agitated until the polymer turned cloudy (~45s). The slide was removed and washed under a stream of distilled water following which it was placed into a bath of developer 50:50 (v/v) Saxby A: Saxby B (Saxby A (6 g 4-(methylamino)phenol sulphate (Metol) and 40 g ascorbic acid in 1 L of water) and Saxby B (100 g anhydrous sodium carbonate and 30 g sodium hydroxide in 1 L of water). The reaction was stopped using 5% (v/v) acetic acid for ~1min. The slide was then rinsed in deionised water and immersed in 10% (v/v) sodium thiosulphate 1:1 (v/v) methanol:water (HYPO) under agitation for ~5min to remove any undeveloped silver bromide (AgBr), and then thoroughly washed with deionised water. The slides were then air dried and placed in a petri dish until the holograms were fabricated.

2.3. Hologram fabrication

A level plastic square container containing a wedge angled at 4° at one end and a silver mirror were used for the ablation process. The glass slide, polymer side facing downwards, was placed into the container with one edge of the slide placed on the wedge (Fig. 1). The container was filled with deionised water and the polymer was exposed to a Nd:YAG pulsed laser (6ns pulse, wavelength 532 nm, spot size ~1cm^2, Q-switch 300–375 μs, ~200 mJ).

Bragg reflection holograms were fabricated as shown Fig. 1. The light, which is scattered by the object (object beam), interferes with the reference beam to form a three-dimensional interference pattern within the polymer Fig. 1(a). Through the chemical development of this medium, the interference pattern is recorded within the volume. The recording (volume hologram) contains all of the information about the original object within the fringe structure [1,20,21]. When illuminated with white light, the VHG selectively filters light according to the Bragg phase-matching condition Fig. 1(b). The simulation of this structure, in the form of its reflection response, is modelled in MATLAB as a 1D periodic, effective medium Bragg stack with varying fill fractions of Ag^0 and AgI nanoparticles in successive layers, with inspiration from Refs. [22–30]. For further details on the modelling methodology see SI.

2.4. Monitoring of holographic response

The ablated polyHEMA slide containing a hologram (75 × 25 mm) was cut into 6 mm sections using a diamond glass cutter to form a batch of sensors for multiple analysis. Individual sensors were inserted into a 4 ml cuvette with the polymer film side facing inward and either used dry or immersed in 1.5 ml deionised water. The 4 ml cuvette was mounted in a cuvette holder

(Knight Photonics, UK), and connected to a fibre optic Avaspec-ULS2048-SLIT-25-VC spectrophotometer (Avantes, UK) with a tungsten halogen white light source Avalight-Hal-S (Avantes, UK) employed to monitor holographic responses. The collimated white light source was focused onto the reverse side of the hologram and the holographic reflection at the Bragg angle was found by adjusting the angles in the cuvette holder. Holographic responses were recorded as peak reflectance intensity at each wavelength in the visible range, using the in-built smoothing and peak detection software AvaSoft 7.2 in reflectance mode, which was connected via a USB cable to a computer.

UV–VIS spectroscopy was undertaken to evaluate changes in the peak plasmon resonance of the silver nanoparticles following exposure to nitric acid. The ablated polyHEMA slide containing a hologram (75 × 25 mm) was cut into 6 mm sections using a diamond glass cutter. Individual sensors were inserted into a 4 ml cuvette with the polymer film side facing inward and 1.5 ml of nitric acid at various molarities added to the cuvette. The spectrometer was set to measure from 200 to 1000 nm with a wavelength interval of 1 nm and a scan speed of 1200 nm/min. An appropriate control was used to blank the system before data collection. Changes in the peak plasmon resonance were measured.

2.5. Rehalogenation protocol

Varying concentrations of nitric and hydrochloric acid were added to the cuvette (1.5 ml) and the changes in wavelength and intensity of the holographic signal were measured over a period of 90min. The acid solution was then completely removed from the cuvette and replaced with an iodine solution (2% (w/v) iodine in 99.8% (v/v) ethanol) until bleaching of the polymer colour occurred and the sensor became transparent. The iodine solution was

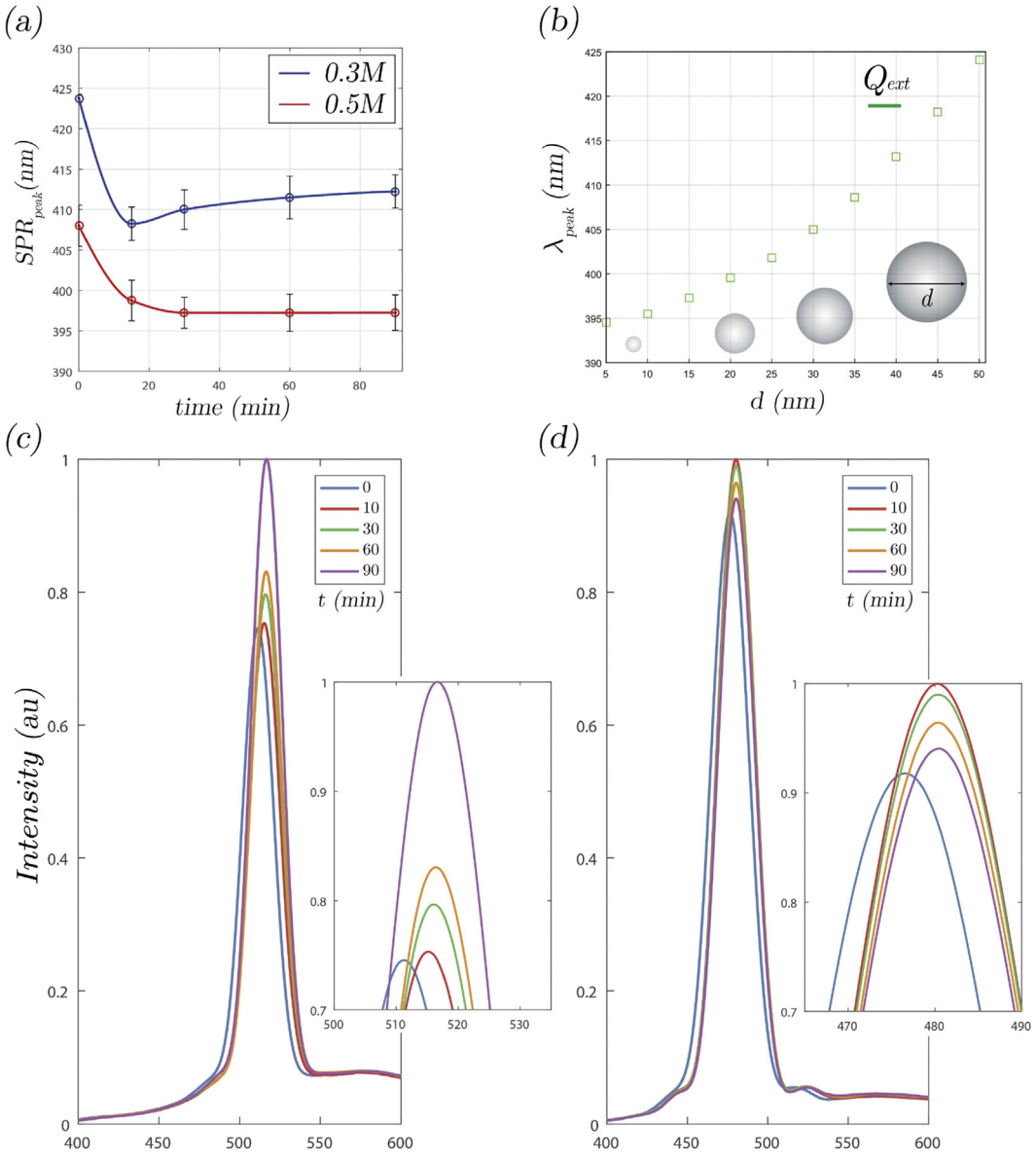

Fig. 2. (a) Average change in the maximum wavelength of the plasmon resonance peak of Ag^0 nanoparticles embedded within a polyHEMA-*co*-DMAEM(7.5%)-co-EDMA (5%) holographic sensor exposed to 0.3 M and 0.5 M HNO3 for a period of 90 min at 23 ± 3 °C. (b) Simulation of extinction cross-section efficiency (Qext) of spherical Ag^0 nanoparticles with varying diameters in background polymer dielectric, with maximum value's spectral position plotted for comparison: MNPBEM toolbox used [31]. Changes in intensity of the holographic signal of a polyHEMA-co–EDMA (5%) sensor (c) and polyHEMA-*co*-DMAEM(7.5%)-co-EDMA (5%) sensor (d) following exposure to 0.5 M nitric acid solution for a period of 90 min at 23 ± 3 °C.

removed and the sensor was washed several times with distilled water. Changes in the holographic replay wavelength and peak intensity were measured using an Avaspec-ULS2048-SLIT-25-VC spectrophotometer and AvaSoft 7.2 software used in reflectance mode.

3. Results & discussion

When VHGs are fabricated by laser ablation and processed according to the methods outlined, the $AgClO_4$ within the polymer matrix is first converted to AgBr and then reduced to Ag^0 nanoparticles with a range of sizes. We hypothesise that this size distribution affects holographic peak intensity by reducing both the efficiency of the grating and the potential for effective refractive index modulation. It is further hypothesised that if the metal nanoparticle size were to be further attenuated, with the smallest particles being solubilised, the fringe structure may become more defined, thereby reducing light scattering and generating a medium more amenable to refractive index modulation.

Attenuation of metal nanoparticles in situ was undertaken by placing VHGs containing Ag^0 nanoparticles embedded in solutions of varying concentrations of HNO_3 for a period of 90min. As measured by UV–VIS spectroscopy at 23 ± 3 °C, the surface plasmon resonance (SPR) peak of Ag^0 nanoparticles embedded in polyhydroxyethylmethacrylate (pHEMA)-*co*-dimethylethylmethacrylate (DMAEM)-*co*-ethylene glycol dimethacrylate (EDMA) polymers changed over a period of 90min, Fig. 2(a). For example, in 0.3 M HNO_3 an average wavelength reduction of 13 nm (equating to a

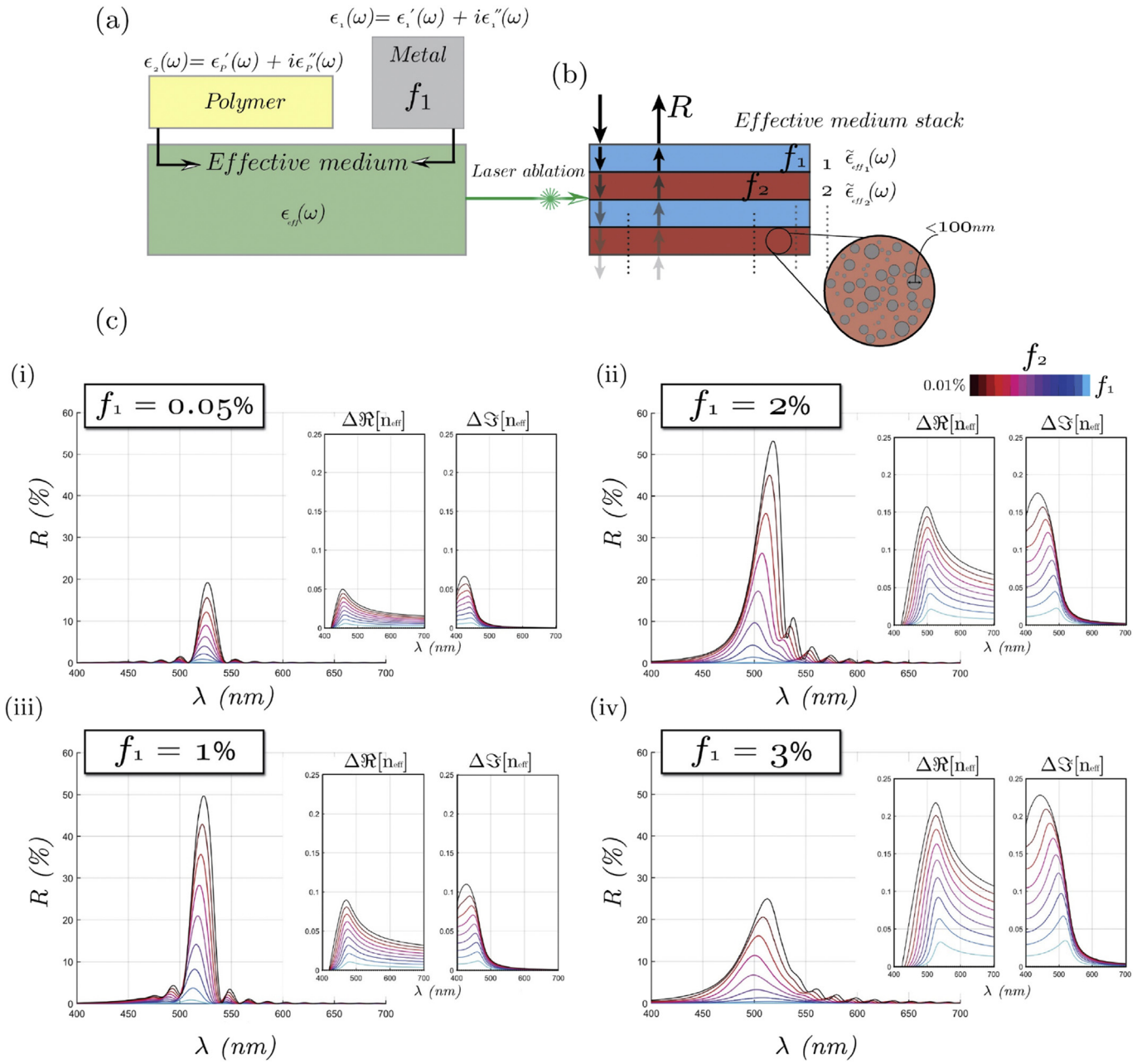

Fig. 3. Simulation of reflection from a 1D Bragg stack, with two effective media as the slabs. Each slab varies fill fraction of silver, f1 and f2. Fill fraction 2, f2, varies from f1 to zero. (a) Reflection using recursive matrix calculations [See ESI for more details], and (b) showing the differential real and imaginary parts of the refractive indices. An optimal fill fraction of between 1.5 and 2% is shown in ESI Fig. S3.C.

reduction of 20 nm in particle size [32]) and a corresponding 20% average reduction in the Full Width at Half Maximum (FWHM) peak) was observed. At all time-points, only a single SPR peak was observed suggesting that the particles remained spherical in nature and similar results were obtained for a variety of hydrophilic polymer chemistries (Sigma Aldrich). Simulation results [31] in Fig. 2(b) (based on the data in ESI Fig. S2), of extinction peak positions of Ag^0 nanoparticles in a background polymer medium, suggest the decrease in SPR peak is an indication of particle size reduction, which agrees with both the consensus view on the interaction of HNO_3 with Ag^0 nanoparticles and classic Mie theory of SPR peak shift with decreasing particle size [35,36]. Thus, the experimental SPR peak temporal shift in Fig. 2(a) can be attributed to a particle size reduction of approximately 15–20 nm. The sensor should not be washed following the etching of particles as nitric acid solubilises the nanoparticles, and leaching into solution or disruption of fringe intensity can occur with the generation of soluble $AgNO_3$.

Spectrophotometric monitoring of the holographic peak intensity of polyHEMA-*co*-EDMA polymers and those with the functional monomer DMAEM, in the presence of 0.5 M HNO_3, exhibit changes in both the replay wavelength and peak intensity of the holographic signal over a period of 90min, Fig. 2(c–d). These changes are believed to be highly dependent on both the metal fill fraction and the nanoparticle size. These issues are highlighted by the suppression of reflection from simulations of a periodic, alternating effective medium, i.e. a 1D stack with varying fill fractions in Fig. 3, and by the simulation results in SI S.3, concerning the effect of the size parameter modification in the Drude term in the dielectric function of Ag^0 to a 1D effective medium stack (see SI).

The simulation results shown in Fig. 3 suggest that a fill fraction differential increase, between successive layers, leads to an expected increase in the refractive index differential around the target green part of the spectra, regardless of the initial fill fraction in the high-index region, and lower imaginary (lossy) part. Along with a slight red-shift, and SPR results in both experimental and simulation methods, one can assert that the acidic environment is likely reducing the particle size and fill fraction of the media. This has an overall effect of increasing refractive index modulation around green wavelengths, minimizing the imaginary part of the index and hence increasing grating efficiency. If there are insufficient particles, or they are too small, a complete loss of the VHG occurs in the presence of acidic conditions. A shift towards longer wavelengths is associated with changes in refractive index, particle size distribution and/or swelling of the matrix.

The formation of soluble $AgNO_3$ is likely to modulate the refractive index under conditions in which the smaller particles within the polymer fringes have been removed, sufficient metal particles are retained and the fringe structure has not been affected by the solubilisation of the metal particles. Evidence to support solubilisation of the Ag^0 was gained by removing the sensor from the acid and washing with distilled water; the holographic signal was completely lost, suggesting that the soluble product had leached from the polymer. It was also possible to demonstrate that a bleaching solution containing a combination of acid and silver halide does not modulate refractive index and causes a decrease in the peak holographic signal. A 0.5 M solution of hydrochloric acid was applied to a polyHEMA-*co*-EDMA sensor for a period of 90min. The acidic environment (pH = 0.67) should solubilise the Ag^0 and convert it to poorly soluble AgCl with a higher refractive index. The results demonstrated a shift in wavelength of ~ −14 nm and a 59% reduction in intensity of the holographic signal. Attempts to modulate the refractive index further using iodine solution yielded a wavelength increase of 8 nm but no increase in the intensity of the holographic signal.

Reversal bleaching is commonly used to modulate refractive index in photochemically produced VHGs by conversion of Ag^0 into a silver halide, but also has the effect of reducing light scattering, as silver halides are almost colourless. Bleaching of nitric acid treated polyHEMA-*co*-EDMA holographic sensor with a 2% (w/v) iodine solution results in a further increase in peak intensity of ~40%. Increases in peak intensity of greater than 200% are obtained when the polymer contains functional groups such as N,N′-dimethylaminoethyl methacrylate (DMAEM) that bind to Ag^0 nanoparticles, Fig. 4(a) [35]. This stability is likely to be important when soluble salts are generated as it may help to retain the silver in the fringes

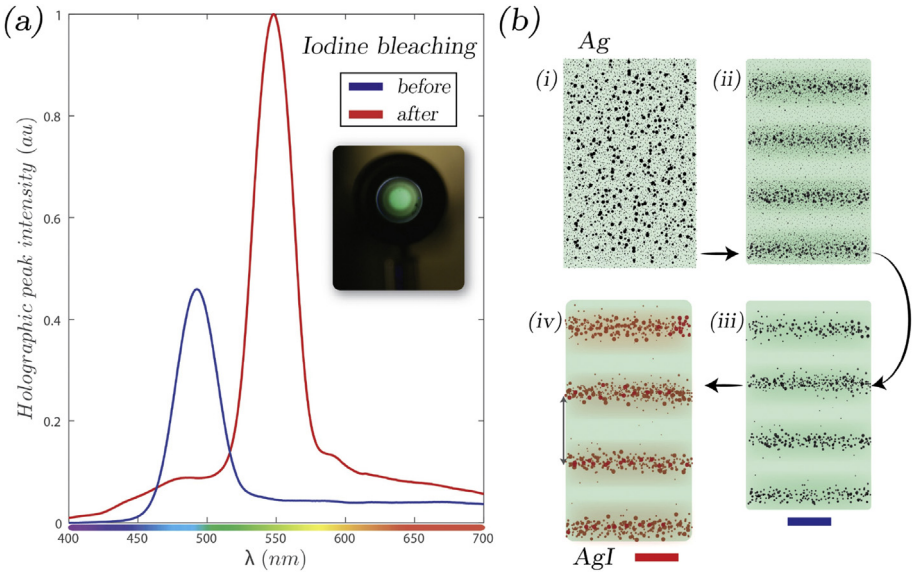

Fig. 4. (a) Intensity changes in the holographic signal of a polyHEMA-*co*-DMAEM 7.5mol% -co-EDMA 5mol% sensor exposed to a 0.5 M nitric acid solution and then bleaching with a 2% (w/v) iodine solution. Inset photograph of the end of a fibre collecting the reflected light from the device. (b) VHG formation process: (i) Ag^0 nanoparticles within a polymer medium prior to ablation (ii) Post laser ablation, Ag^0 nanoparticle formation, with spatial and size distribution, formed throughout medium from two wave interference (iii) Introduction of nitric acid solution which is thought to reduce size of Ag^0 particle hence removing smaller particles and reducing size of larger particles (iv)Iodine bleaching: forms AgI at nanoparticle sites, increasing the particle size, fill fraction and resulting in fringe spacing expansion.

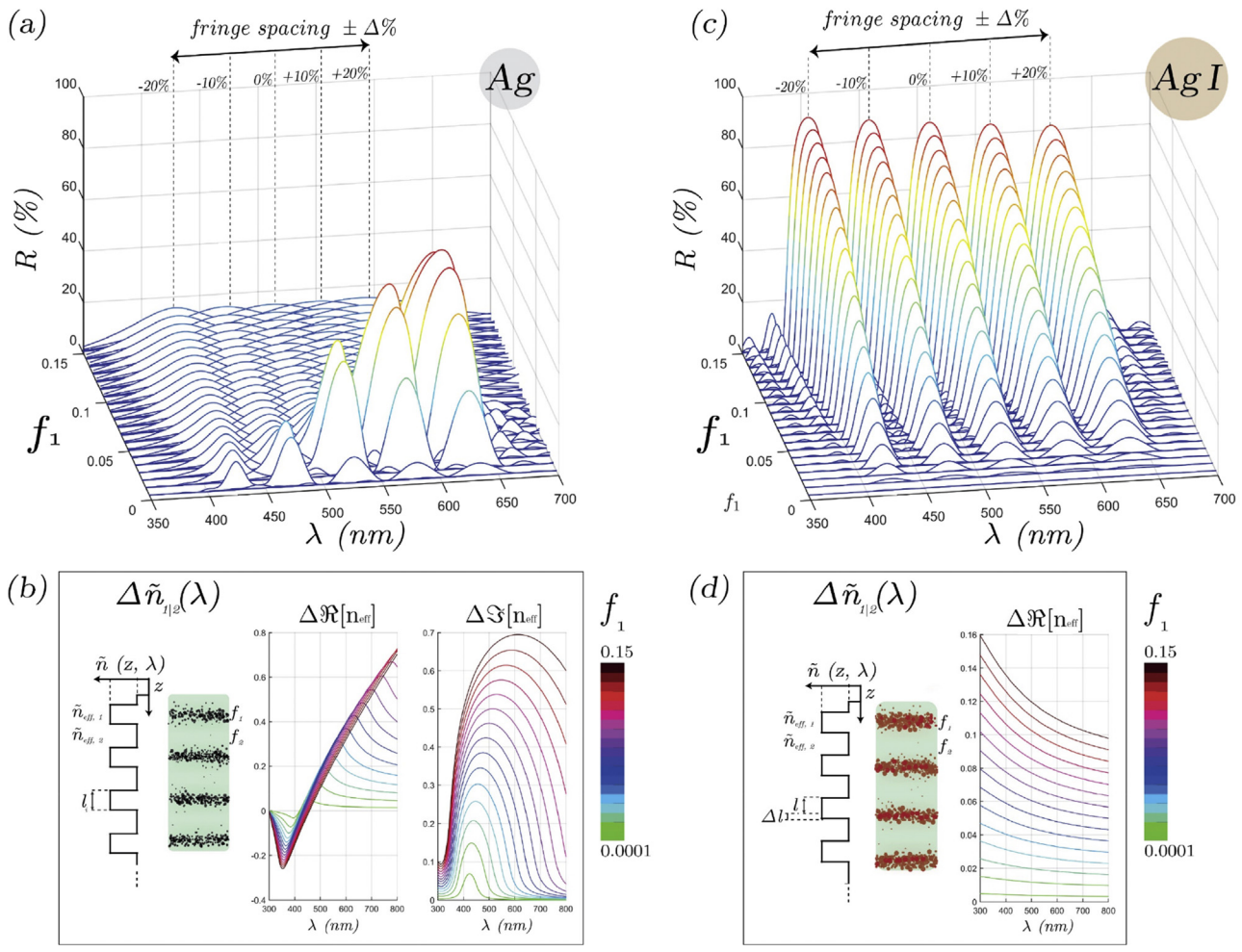

Fig. 5. Simulations of adjustment of fill fraction of (a) Ag and (c) AgI, inclusions in background polymer using EMT and recursion relations for $N = 20$ bi-layers (terminated on a glass medium), with varying fringe spacing thicknesses. (b) and (d) show the real and imaginary part of the refractive index differential between $n_{\text{eff},1}$ and $n_{\text{eff},\,2}$ layers of Ag and AgI respectively. In addition, a schematic of the refractive index profile (at one wavelength) in relation to the stack is illustrated. For further details, see SI S3.

during the bleaching process when soluble salts are generated. If these salts are not protected in the acidic environment, some movement of Ag^+ ions may occur into solution, which would disrupt fringe integrity. DMAEM contains a tertiary amino ($-N(CH_3)_2$) pendant group, which can accept protons in response to increasing acidity. A rapid alteration of the net charge of the pendant group causes an alteration of the hydrodynamic volume of the polymer and a transition from collapsed to an expanded state, which is occasioned by the osmotic pressure exerted by mobile counter-ions that neutralise the network charges [36].

If a polyHEMA-*co*-DMAEM (7.5mol%)-co-EDMA (5%) holographic sensor is left in 0.5 M HNO_3 for 120 min, the wavelength of the holographic signal increases by ~55 nm and the peak intensity reduces to ~ 10% of the original signal and completely disappears by 360min. When the holographic sensor is removed from the 0.5 M HNO_3 solution at 90min and then placed into a 2% (w/v) iodine solution until bleached, the wavelength of the holographic peak intensity increases by >200% and there is an associated red-shift in wavelength (Fig. 4 (a)). This increase translates into a signal intensity that is observable in ambient lighting in the case of a polyHEMA-*co*-DMAEM (7.5mol%)-co-EDMA (5mol%) holographic sensor. The entire process of VHG formation is illustrated in the schematic shown in Fig. 4(b).

The chemical transformation of Ag^0 to AgI inclusions is known to increase particle size, fill fraction of inclusions and fringe expansion. This action experimentally translates into two changes in the holographic peak signal: a red shift and significant intensity increase. To assist the explanation of this experimental data, simulation results in Fig. 5, highlight how the effect of varying the fill fraction of either Ag^0 or AgI inclusions (experimentally due to the iodine bleaching) while adjusting the fringe spacing (i.e. expansion/contraction), modifies the reflection response. Firstly, increasingly large volumes of silver inclusions eventually mean a percolation threshold is reached due to the increasing imaginary component, Fig. 5(c), which results in considerable loss. However, with an adequate Ag^0 fill fraction, a chemical transformation to AgI, which as a material is usually considered a very weakly absorbing medium with negligible extinction in the visible spectrum [37], results in the combination of a refractive index differential (real part) sufficient to provide a good reflection response in the target spectral region, negligible loss and thus because of many periodic layers, a large total reflection from the stack. In addition, the significant experimental red shift can be attributed to the expansion of the fringe spacing.

4. Conclusions

Nitric acid has been shown to etch the size of the Ag^0 nanoparticles within the polymer matrix, which is hypothesised to generate more distinct fringes amenable to refractive index

modulation. The protocol outlined in this research, whereby the ablated VHG is first immersed in nitric acid followed by a silver halide transformation, has demonstrated the ability to increase significantly the peak holographic signal intensity to levels that are visible in ambient lighting. To explain this behaviour, a periodic effective medium, 1D Bragg stack simulation methodology is used. Incorporation of a functional monomer that binds the metal nanoparticles increases the potential for increasing signal intensity, which is thought to stabilize the particles and reduce the chances of loss of fringe integrity. These results provide substantial theoretical and practical implications for the design of simple and affordable diagnostics that provide rapid analysis without the need for laboratory equipment.

Acknowledgements

EPSRC Integrated Photonics and Electronic Systems (Grant number: EP/L015455/1) Centre for Doctoral Training.

Appendix A. Supplementary data

Supplementary data related to this article can be found at http://dx.doi.org/10.1016/j.optmat.2017.08.003.

References

[1] Y.N. Denisyuk, Photographic reconstruction of the optical properties of an object in its own scattered radiation, Dokl. Akad. Nauk. SSSR 144 (1962) 1275–1278.
[2] E.N. Leith, J. Upatnieks, Reconstructed wavefronts and communication theory, J. Opt. Soc. Am. 52 (1962) 1123.
[3] J.L. Martinez-Hurtado, C.A.B. Davidson, J. Blyth, C.R. Lowe, Holographic detection of hydrocarbon gases and other volatile organic compounds, Langmuir 26 (19) (2010) 15694–15699.
[4] A.G. Mayes, B. Blyth, M. Kyröläinen-Reay, R.B. Millington, C.R. Lowe, A holographic alcohol sensor, Anal. Chem. 71 (16) (1999) 3390–3396.
[5] H. Blyth, R.B. Millington, A.G. Mayes, E.R. Frears, C.R. Lowe, Holographic sensor for water in solvents, Anal. Chem. 68 (7) (1996) 1089–1094.
[6] A.G. Mayes, J. Blyth, R.B. Millington, C.R. Lowe, Metal ion-sensitive holographic sensors, Anal. Chem. 74 (15) (2002) 3649–3657.
[7] A.J. Marshall, J. Blyth, C.A.B. Davidson, C.R. Lowe, pH-sensitive holographic sensors, Anal. Chem. 75 (17) (2003) 4423–4431.
[8] B.M. González, G. Christie, C.A.B. Davidson, J. Blyth, C.R. Lowe, Divalent metal ion-sensitive holographic sensors, Anal. Chim. Acta 528 (2005) 219–228.
[9] C.A.B. Davidson, J. Blythe, C.R. Lowe, Method of Production of a Holographic Sensor, W2010041079 A1, April 15, 2010.
[10] A.K. Yetisen, I. Naydenova, F. da Cruz Vasconcellos, J. Blyth, C.R. Lowe, Chem. Rev. 114 (2014) 10654–10696.
[11] H.A. Macleod, Thin-film Optical Filters, Institute of Physics Publishing, 2001.
[12] S.J. Orfanidis, Electromagnetic Waves and Antennas, Rutgers University, Piscataway, NJ, 2008.
[13] E. Lidorikis, S. Egusa, J.D. Joannopoulos, Effective medium properties and photonic crystal superstructures of metallic nanoparticle arrays, J. Appl. Phys. 101 (2007) 054304.
[14] Harman Technology, Harman Technology Limited, 2007. http://www.harmantechnology.com/Technology/Holography/tabid/182/Default.aspx.
[15] C.R. Lowe, C. Larby, Holography gets smart, Phys. World (Feb 2008). http://physicsworld.com/cws/article/print/2008/feb/01/holography-gets-smart.
[16] P. Hariharan, C.M. Chidley, Rehalogenating bleaches for photographic phase holograms. 2: spatial frequency effects, Appl. Opt. 27 (1988) 3852–3854.
[17] C. Ozmetin, M. Copur, A. Yartasi, M.M. Kocakerim, Kinetic investigation of reaction between metallic silver and nitric acid solutions in the range 7.22–14.44 M, Ind. Eng. Chem. Res. 37 (1998) 4641–4645.
[18] S.K. Sadrnezhaad, E. Ahmadi, M.J. Mozammel, Kinetics of silver dissolution in nitric acid from Ag-AU(0.04)-CU0.10 and Ag–Cu-0.23 scraps, J. Mater. Sci. Technol. 22 (2006) 696–700.
[19] S. Elzey, V.H. Grassian, Agglomeration, isolation and dissolution of commercially manufactured silver nanoparticles in aqueous environments, J. Nanopart. Res. 12 (2010) 1945–1958.
[20] G. Saxby, Manual of Practical Holography, Butterworth-Heinemann Ltd, 1991.
[21] H.M. Smith, Principles of Holography, John Wiley & Sons, London, 1975.
[22] E. Lidorikis, S. Egusa, J.D. Joannopoulos, Effective medium properties and photonic crystal superstructures of metallic nanoparticle arrays, J. Appl. Phys. 101 (2007) 054304G.
[23] A. Niklasson, C.G. Granqvist, O. Hunderi, Effective medium models for the optical properties of inhomogeneous materials, Appl. Opt. 20 (1981) 26–30.
[24] M.L. Protopapa, Simulation of optical properties of layered metallic nanoparticles embedded inside dielectric matrices: interference method or Maxwell Garnett effective-medium theory? Appl. Opt. 49 (16) (2010) 3014–3024.
[25] W.T. Doyle, Optical properties of a suspension of metal spheres, Phys. Rev. B 39 (1989) 9852–9858.
[26] A.D. Rakic, A.B. Djurisic, J.M. Elazar, M.L. Majewski, Optical properties of metallic films for vertical-cavity optoelectronic devices, Appl. Opt. 37 (1998) 5271–5283.
[27] K.R. Sui, X.S. Zhu, X.L. Tang, K. Iwai, M. Miyagi, Y.W. Shi, Method for evaluating material dispersion of dielectric film in the hollow fiber, Appl. Opt. 47 (2008) 6340–6344.
[28] S.K. Ghosh, T. Pal, Interparticle coupling effect on the surface plasmon resonance of gold nanoparticles: from theory to applications, Chem. Rev. 107 (2007) 4797–4862.
[29] J. Lekner, Reflection by absorbing periodically stratified media, J. Opt. 16 (3) (2014) 035104.
[30] D. Aspnes, Local-field effects and effective-medium theory: a microscopic perspective, Am. J. Phys. 50 (1981) 704–709.
[31] U. Hohenester, A. Trügler, MNPBEM - a Matlab toolbox for the simulation of plasmonic nanoparticles, Comput. Phys. Commun. 183 (2) (2012) 370–381.
[32] Sigma Aldrich, Silver Nanoparticles: Properties and Applications, 2015.
[35] L.V. Trandafilovic, A.S. Luyt, N. Bibic, S. Dimitrijevic-Brankovic, M.K. Georges, T. Radhakrishnan, V. Djokovic, Formation of nano-plate silver particles in the presence of polyampholyte copolymer, Colloids Surf. A Physiochem. Eng. Asp. 414 (2012) 17–25.
[36] E.S. Gil, S.M. Hudson, Stimuli-responsive polymers and their bioconjugates, Prog. Polym. Sci. 29 (2004) 1173–1222.
[37] G.J. Cochrane, Some optical properties of single crystals of hexagonal silver iodide, Phys. D. Appl. Phys. 7 (1974).